ELSEVIER

Biomaterials 23 (2002) 1073–1080

Biomaterials

www.elsevier.com/locate/biomaterials

Calcium phosphate apatites with variable Ca/P atomic ratio II. Calcination and sintering

S. Raynaud, E. Champion*, D. Bernache-Assollant

Science des Procédés Céramiques et de Traitements de Surface, UMR 6638, 123, Avenue Albert Thomas, 87060 Limoges Cedex, France

Received 1 December 2000; accepted 11 June 2001

Abstract

The calcination and natural sintering of calcium deficient hydroxyapatite powders $Ca_{10-x}(PO_4)_{6-x}(HPO_4)_x(OH)_{2-x}$ (with $0 \leqslant x \leqslant 1$) were studied. For temperature below 700°C, particle coalescence occurs without densification. The particle coalescence is associated with a reduction of the specific surface area. This surface decreases all the more as the Ca/P molar ratio of the powder is small. The mechanism agrees with a transfer of matter occurring by superficial diffusion, which is enhanced by the augmentation of vacancies in the apatitic structure (i.e. by a decrease of the Ca/P ratio). The sintering of compacted powders begins at 700°C. At the same temperature, the calcium deficient hydroxyapatites dissociate into biphasic mixtures of hydroxyapatite and tricalcium phosphate. The sintering is slowed down when the content of TCP in the biphasic mixture increases. In parallel, the grain size increases. This result relates to the augmentation of the coalescence of particles at low temperature.

Keywords: Hydroxyapatite; Tricalcium phosphate; Calcination; Sintering

1. Introduction

This paper is the second part of the study devoted to the elaboration and characterisation of apatitic calcium phosphate based materials. From the hydroxyapatite structure (HAP) $Ca_{10}(PO_4)_6(OH)_2$ many ion substitutions are possible. The substitution of phosphate ions (PO_4^{3-}) by hydrogenophosphate ones (HPO_4^{2-}) allows a continuous variation of the Ca/P atomic ratio between 9/6 and 10/6 [1]. This leads to calcium deficient hydroxyapatites (Ca-dHAP) $Ca_{10-x}(PO_4)_{6-x}(HPO_4)_x(OH)_{2-x}$, with $0 \leqslant x \leqslant 1$. Ca-dHAP powders can be precipitated from conventional wet chemical methods and decomposed into a mixture of HAP and tricalcium phosphate $Ca_3(PO_4)_2$ –TCP- by thermal treatment above 700°C. This allows a direct processing of biphasic calcium phosphate ceramics HAP/TCP without the step of powder blending. Ceramic parts processing includes high temperature treatments of sintering and it is known that important changes may occur in powder compacts at temperatures inferior to that required to activate the densification mechanisms. It was demonstrated that surface reduction may occur in HAP powders by particle coalescence without sintering [2], which is detrimental for the subsequent densification. Moreover, the proportion of HAP and TCP in the biphasic mixture after decomposition of the initial Ca-dHAP may also influence greatly the sintering and the final microstructure of the ceramics.

The present paper is concerned with the calcination of Ca-dHAP powders and with the natural sintering of polyphasic calcium phosphate ceramics. The aim was to investigate the influence of hydrogenophosphate substitution in the apatite lattice on the decrease of specific surface area of Ca-dHAP powders according to the temperature, and to evaluate the influence of phase proportions on the sintering of the polyphasic calcium phosphate mixtures issued from the thermal decomposition of these Ca-dHAP powders.

2. Experimental methods

Powders with variable Ca/P molar ratios were investigated. Synthesis conditions are detailed in part I

*Corresponding author. Tel.: +33-05-55-45-74-60; fax: +33-05-55-45-75-86.

E-mail address: champion@unilim.fr (E. Champion).

0142-9612/02/$ - see front matter
PII: S0142-9612(01)00219-8

of the study. The main characteristics, Ca/P molar ratio, initial specific surface area and phase constitution of powders, are summarised in Table 1.

In a first step, the powders were calcined between 400°C and 1000°C for 30 min to determinate the surface reduction according to the temperature. The surface area was measured by the BET method, 8 points (analyzer Micromeritics ASAP 2010) after degassing under vacuum at 200°C. Then, for the kinetic approach of surface reduction, powders were heated for 0 min to 4 h in the 400–700°C temperature range under isothermal conditions. To this end, powders were introduced in the furnace at the calcination temperature and taken off after the holding time.

For sintering experiments, powders were initially heated to reach a same specific surface area of $30\,m^2\,g^{-1}$. This initial treatment is of prime importance because the sintering kinetics depend on both the chemical composition of the powder and the grain surface. Earlier studies did not take this into account so that confusion exists between the effect of surface and that of composition on the sintering behaviour [3,4]. Starting from the same surface area allowed us to characterise the effects of the chemical composition on the sintering.

After the initial heat treatment, the powders were pressed in a cylindrical die under a compressive stress of 120 MPa. The compaction ratio of the samples was 42%. Linear shrinkage was measured by dilatometry (Setaram TMA 92, France). The thermal cycle included a 30 min holding time at 1250°C and the heating and cooling rates were $5°C\,min^{-1}$ and $10°C\,min^{-1}$, respectively.

The relative density of sintered materials was measured by the Archimedean method in water. Secondary electron microscopy (Philips XL 30) was used for morphological observations. To reveal the microstructure, the surface of sintered samples was mirror-polished and thermally etched at 1220°C for 3 min prior to the observation.

Phases analyses were determined by powder X-ray diffraction (XRD) using procedures similar to those described in part I of the study.

3. Results and discussion

3.1. Determination of the different domains of surface reduction

Fig. 1 gives typical evolutions of the specific surface area of powders versus temperature. Plots are normalised with regard to the surface area determined at 400°C. Only very low surface decreases were noted below 500°C. Above this temperature, the reduction of surface increased strongly. It reached a maximum rate between 600°C and 800°C. At higher temperature the rate of surface reduction slowed down.

Fig. 2 shows linear shrinkage of samples versus temperature. Shrinkage began from 700°C. Below that temperature samples expanded in agreement with a thermal expansion coefficient comprised between 12×10^{-6} and $16\times10^{-6}\,K^{-1}$, values that correspond to the thermal expansion coefficients of calcium phosphate apatites [5,6]. This means that the reduction of specific surface area measured between 400°C and 700°C corresponds to particle coalescence without densification process. Therefore, two domains must be distinguished. The first one is associated with the calcination for temperatures up to 700°C, and the

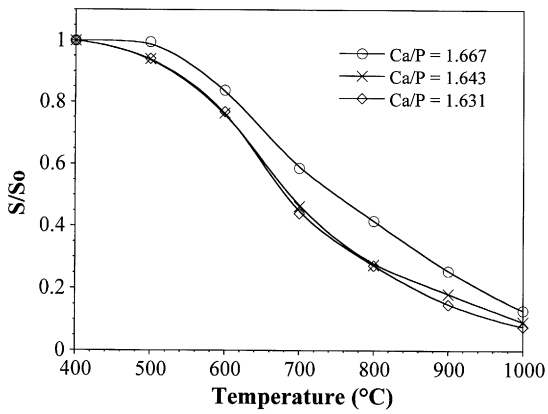

Fig. 1. Normalised surface area versus calcination temperature (30 min holding time).

Table 1
Characteristics of calcium phosphate powders

Ca/P molar ratio	S_0 ($m^2\,g^{-1}$)	Powder composition ($T < 700°C$)
1.44 ± 0.02	88 ± 2	$Ca_9(HPO_4)(PO_4)_5(OH) + CaHPO_4$
1.535 ± 0.004	47 ± 0.5	$Ca_{10-x}(HPO_4)_x(PO_4)_{6-x}(OH)_{2-x}$; $x = 0.79$
1.631 ± 0.004	68 ± 1.5	$Ca_{10-x}(HPO_4)_x(PO_4)_{6-x}(OH)_{2-x}$; $x = 0.21$
1.644 ± 0.002	62 ± 1.5	$Ca_{10-x}(HPO_4)_x(PO_4)_{6-x}(OH)_{2-x}$; $x = 0.14$
1.659 ± 0.001	63 ± 1.5	$Ca_{10-x}(HPO_4)_x(PO_4)_{6-x}(OH)_{2-x}$; $x = 0.05$
$1.667^{+0.005}_{-0.001}$	58 ± 1.3	$Ca_{10}(PO_4)_6(OH)_2$
1.71 ± 0.01	55 ± 1	$Ca_{10}(PO_4)_6(OH)_2 + Ca(OH)_2$

second one is associated with the sintering above that temperature, domain in which densification mechanisms occur.

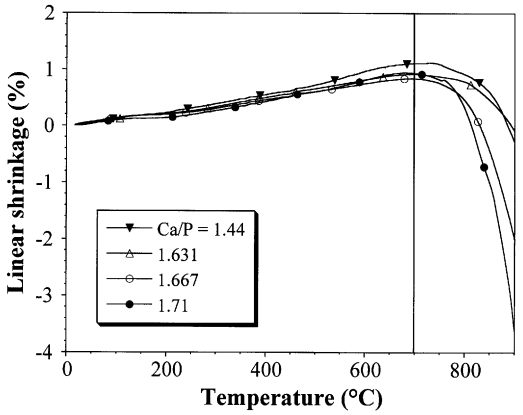

Fig. 2. Linear shrinkage versus temperature (heating rate 5°C min^{-1}).

3.2. Calcination of powders at $T \leqslant 700°C$

3.2.1. Morphological observations

The morphology of powders after different calcination treatments are given in Fig. 3. Whereas initial powders were constituted of small agglomerated needle-like crystals (Fig. 3a), the calcination led to more rounded particles and to the formation of necks between these particles (Fig. 3b and c). These phenomena corresponded to a coalescence of particles that was all the more important as the Ca/P ratio of the powder was decreased. After heating at 700°C for 4 h, the strongest coalescence was observed in the powder with Ca/P = 1.44 (Fig. 3d). In this powder, initial crystals were no more distinguishable, they have coalesced to form grains of tortuous morphology with dimensions that could reach 1 μm. This structure should result from several successive steps. The first one is the formation of necks between particles. The second one corresponds to a

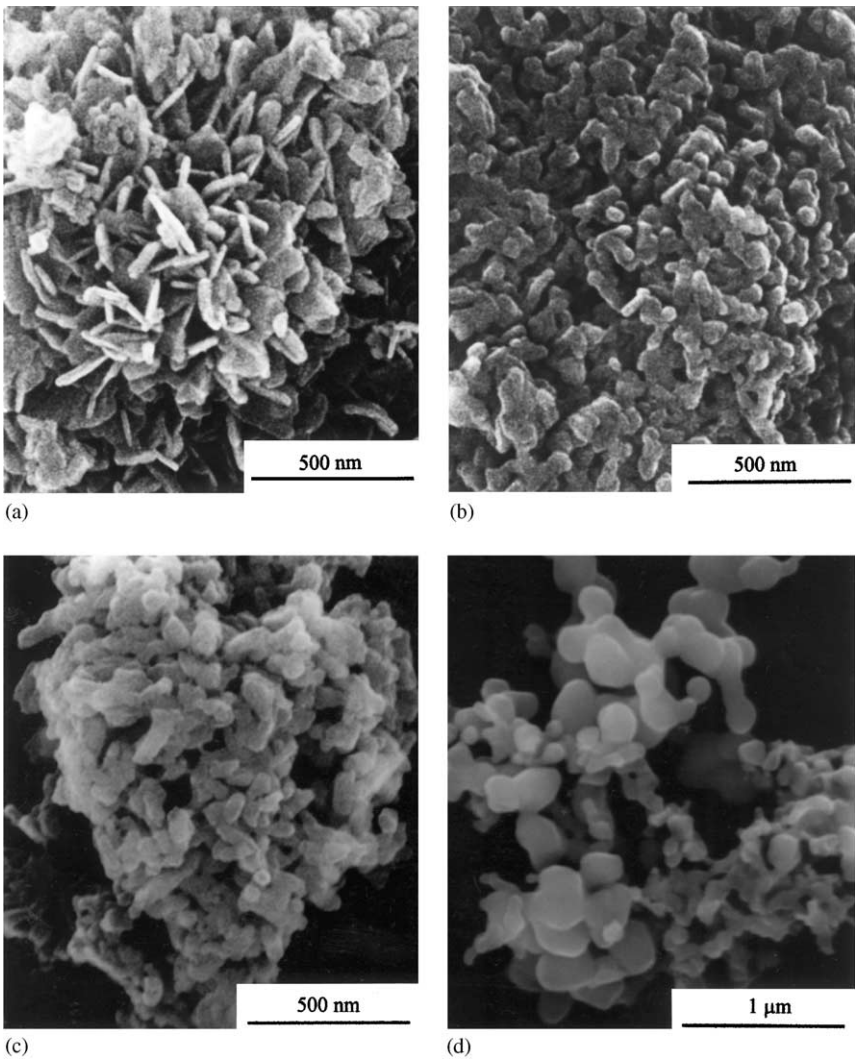

Fig. 3. SEM micrographs of powders. (a) Ca/P = 1.631 as synthesised; (b) Ca/P = 1.631 calcined 650°C–2 h; (c) Ca/P = 1.667 calcined 700°C–4 h; (d) Ca/P = 1.44 calcined 700°C–4 h.

diffusion of matter between the bounded grains from the smaller grains near the greater ones. In this case, there is a displacement of the grain boundary that results in the formation of a porous network. A similar behaviour was already described in other ceramic powders [7]. On the opposite, in the powder with Ca/P = 1.667, and for the same thermal treatment, crystals remained of small size (about 100 nm) with a spherical-like morphology (Fig. 3c). From these observations, it can be assessed that the coalescence of particles occurs in three successive steps, rounding of particles, formation of necks at particles contacts and coalescence of these particles at a rate that appears increasing as the Ca/P ratio of the initial powder decreases.

3.2.2. Kinetic of surface reduction

Different models of grain growth kinetic have been established in the literature. A combination of several approaches leads to an expression of the rate of surface reduction according to an exponential law [8–12]

$$dS/dt = kS^m, \quad (1)$$

where S is the surface area, k a temperature dependent kinetic constant and m the surface exponent, which is characteristic of the mechanism responsible for the reduction of surface area.

As shown by Hébrard [12], this equation can be deduced from the derivative of the following mathematical expression:

$$S = St_0(1 + At)^n, \quad (2)$$

where S is the surface area at time t, St_0 the initial surface area, A and n are constants.

The derivative of Eq. (2) allows to identify the constants m and k of Eq. (1) as

$$m = 1 - 1/n,$$

$$k = nASt_0^{1/n}.$$

If the reduction of surface occurs without densification m is equal to 6 or 8 when the mechanism is evaporation-condensation or superficial diffusion, respectively [8]. Therefore, the exponent n of Eq. (2) must be equal to –1/5 or –1/7.

Fig. 4 (a and b) gives typical isothermal evolution of surface area at 600°C, 650°C and 700°C for powders with different Ca/P ratios. Dots are experimental values and line drawings represent Eq. (2) fitted to experimental data. Table 2 gives the values of St_0 and A determined from the fitting of Eq. (2) with $n = -1/7$. For all the compositions, $n = -1/7$ corresponded to the highest correlation coefficients except for the powder with Ca/P = 1.71. The value $n = -1/7$ corresponds to $m = 8$ and means that the reduction of surface area would occur through a matter transfer by a mechanism of superficial diffusion.

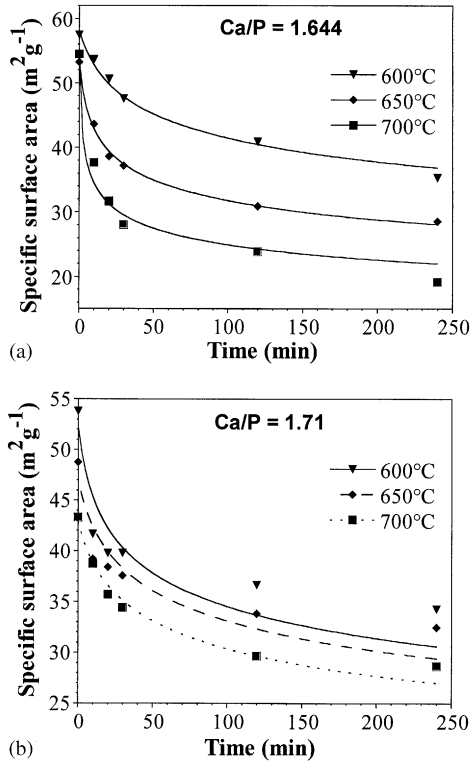

Fig. 4. Surface area of calcium phosphate powders versus calcination time. (a) Ca/P = 1.644; (b) Ca/P = 1.71.

Table 2
Fitting parameters of Eq. (2): $S = St_0(1 + At)^{-1/7}$, during isothermal calcination of powders (R: correlation coefficient)

Ca/P	T = 600°C			T = 650°C			T = 700°C		
	St_0 ($m^2 g^{-1}$)	A	R	St_0 ($m^2 g^{-1}$)	A	R	St_0 ($m^2 g^{-1}$)	A	R
1.44	76.9±1.6	0.12 ±0.03	0.99	75.8±2.6	1.96 ±0.6	0.99	63.3±5.7	37 ±37	0.96
1.535	49.8±1.6	0.18 ±0.06	0.98	46 ±1.5	2.34 ±0.7	0.99	39.2±1.5	16 ±6.5	0.99
1.631	59.8±1.4	0.06 ±0.02	0.99	55.2±0.9	0.22 ±0.04	0.99	54.5±3.6	2.52±1.6	0.98
1.644	58.1±0.1	0.01 ±0.02	0.99	53.3±0.6	0.36 ±0.04	0.99	54.5±2.3	2.39±0.9	0.99
1.659	54.7±1.6	0.09 ±0.03	0.99	51 ±1.1	0.18 ±0.04	0.99	50.4±1.1	0.62±0.13	0.99
1.667	46.8±0.4	0.009±0.001	0.98	43.2±1	0.025±0.008	0.97	43.2±2.1	0.11±0.06	0.98
1.71	52.2±3.2	0.17 ±0.2	0.89	46.7±2.5	0.10 ±0.06	0.91	42.9±0.9	0.10±0.02	0.98

For the powder with Ca/P = 1.71 calcined at 600°C and 650°C, a value of $n = -1/13$ allowed the best fitting. This would mean that $m = 14$, value that does not correspond to any mechanism according to the above mentioned models. The presence of two phases (98.5 wt% HAP and 1.5 wt% $Ca(OH)_2$) and the dehydroxylation of $Ca(OH)_2$ that occurs in this temperature range could explain the lack of significance of the model.

For powders having Ca/P $\leqslant$ 1.667, the experimental results agreed well with the model at 600°C and 650°C but deviated from the regressions at 700°C. The calculated values of the rate constant k are plotted in Fig. 5. At 600°C and 650°C, k increased slowly with the temperature increase and with the decrease of the Ca/P ratio of the powder. At 700°C, these variations became highly marked. Up to 650°C, the increase of surface reduction with the decrease of Ca/P ratio can be explained by the augmentation of ionic vacancies (V''_{Ca} and V°_{OH}) present in Ca-dHAP $Ca_{10-x}(V''_{Ca})_x(HPO_4)_x(PO_4)_{6-x}(OH)_{2-x}(V^{\circ}_{OH})_x$. The vacancies make the transfer of matter easier, enhancing the particle coalescence. But, at 700°C this approach cannot be used because several changes occur that can explain the deviation of the fitted equation from the experimental data. As shown on the XRD patterns of calcined powders (Fig. 6), the Ca-dHAP phase was stable up to 650°C whereas it dissociated into HAP and TCP at 700°C. Moreover, the sintering begins at 700°C. So, densification must be taken into account of the surface reduction from 700°C. Therefore, the reduction of surface area cannot be described using the laws used in the model previously described, which was established for single phase particle coalescence without densification. The analysis should integrate the densification in biphasic systems, the kinetic of the chemical transformation of the initial apatite and the surface area of particles resulting from this decomposition. This approach has not been investigated in this work.

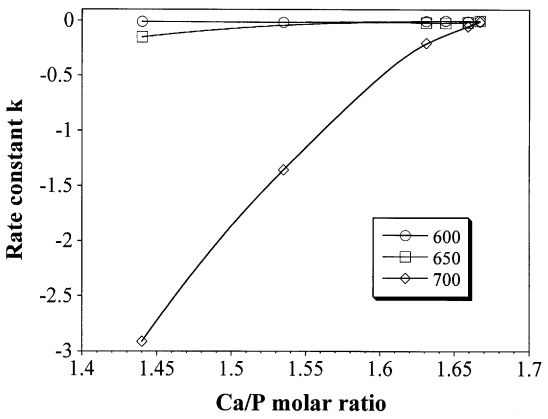

Fig. 5. Calculated rate constant k during isothermal surface reduction.

3.3. Sintering

The starting surface area of powders and the associated calcination conditions are given in Table 3. The temperature of the initial calcination was chosen below 700°C to preserve the single phased Ca-dHAP before the dilatometric experiment. Fig. 7 gives the linear shrinkage of samples during the thermal cycle. The sintering began at 700°C and above that tempera-

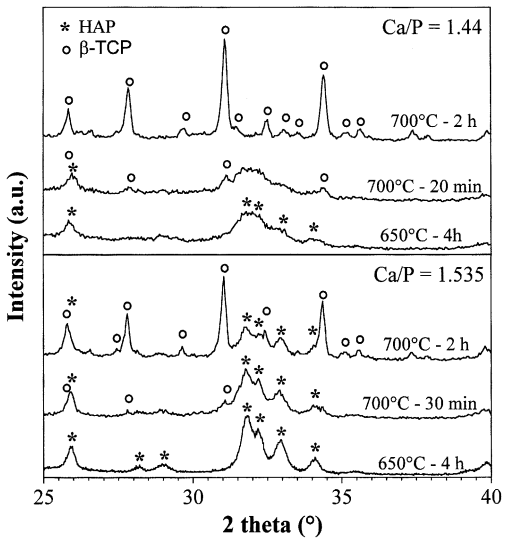

Fig. 6. XRD patterns of powders (Ca/P = 1.44 & Ca/P = 1.535) after different treatments of calcination.

Table 3
Calcination conditions and resulting specific surface area of powders and composition of calcium phosphates at high temperature

Ca/P molar ratio	Calcination conditions (min)	S ($m^2 g^{-1}$)	Composition at $T > 700$°C (wt%)
1.44 ±0.02	650°C–120	31.3±0.3	TCP (90) + $Ca_2P_2O_7$ (10)
1.535±0.004	600°C–180	32.5±0.4	TCP (77) + HAP (23)
1.631±0.004	650°C–120	30.0±0.2	TCP (20) + HAP (80)
1.644±0.002	650°C–120	29.6±0.2	TCP (13) + HAP (87)
1.659±0.001	650°C–210	30.3±0.2	TCP (4.5) + HAP (95.5)
$1.667^{+0.005}_{-0.001}$	700°C–60	29.3±0.2	HAP (>99.5)
1.71 ±0.01	700°C–60	31.2±0.3	HAP (98.5) + CaO (1.5)

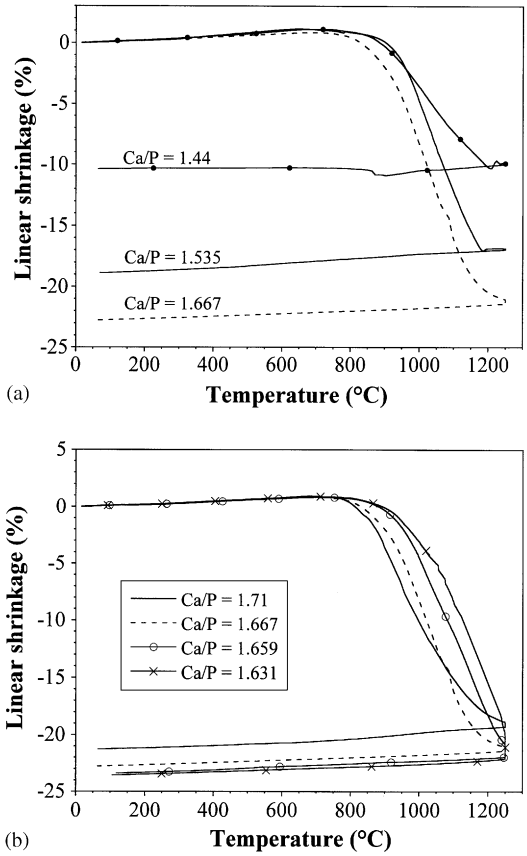

Fig. 7. Linear shrinkage versus temperature. (a) pure HAP (Ca/P = 1.667) and HAP/TCP biphasic materials with a high amount of TCP; (b) HAP/TCP biphasic materials with a low amount of TCP and HAP/CaO biphasic material (Ca/P = 1.71).

ture the initial Ca-dHAPs were decomposed into biphasic calcium phosphates whose compositions are given in Table 3. Biphasic compounds had a lower shrinkage rate than pure HAP (Ca/P = 1.667). For biphasic materials HAP/TCP with a high amount of TCP (i.e. Ca/P = 1.44 and 1.531 in Fig. 7a) a dilatometric accident occurred between 1150°C and 1200°C with an expansion of the sample. This sudden change, already described in the literature [6], was ascribed to the allotropic transformation of β-TCP into α-TCP, which is associated with a theoretical volume increase of about 7% and explains the registered expansion. After sintering, the total linear shrinkage was below 20% and remained much smaller than the one observed for stoichiometric HAP. The expansion accompanying the allotropic transformation of the TCP phase was not observable in HAP/TCP materials containing a low amount of TCP (TCP < 30 wt%, 1.63 < Ca/P < 1.667, Fig. 7b) and though the shrinkage rate was lower than that of pure HAP, the final linear shrinkage after cooling was about 24% and close to that of pure HAP. The biphasic material HAP/CaO behaved similar to HAP, only a small diminution of the shrinkage was observed after the thermal treatment (Fig. 7b).

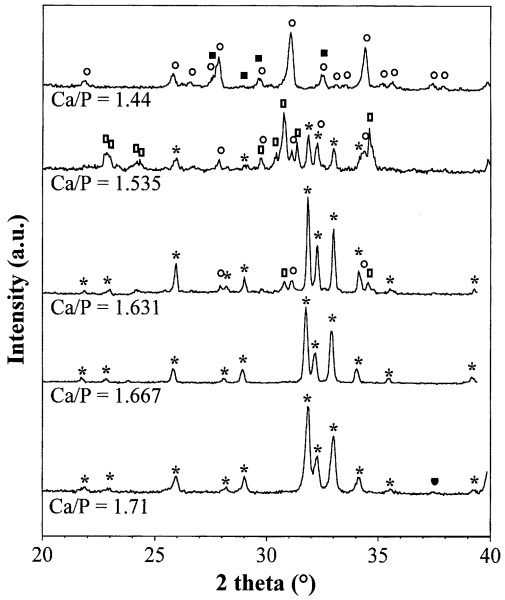

Fig. 8. XRD patterns of sintered materials (referred to the initial Ca/P molar ratio). (*) HAP; (°) β-TCP; (□) α-TCP; (●) CaO; (■) β-$Ca_2P_2O_7$.

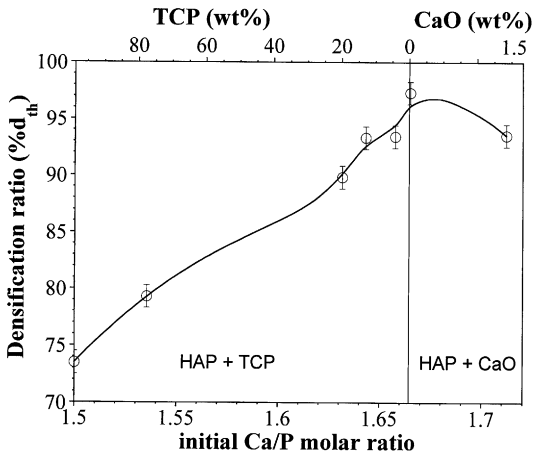

Fig. 9. Densification ratio of sintered materials (1250°C–30 min).

XRD patterns of sintered materials (Fig. 8) showed that biphasic mixtures of HAP and TCP contained both α-TCP and β-TCP, which means that the allotropic transformation of TCP was not totally reversed during cooling. The final densification ratio of sintered materials is given in Fig. 9. It was maximum for HAP at 97% of the theoretical density. It was slightly lower, at 93.5%, in the presence of a small amount of CaO in the HAP matrix and it dropped strongly with the increase of TCP loading in HAP/TCP materials. It was below 90% of the theoretical density when the amount of TCP was more than 20 wt%. These results confirmed the lower sinterability of biphasic compounds in comparison with the stoichiometric HAP.

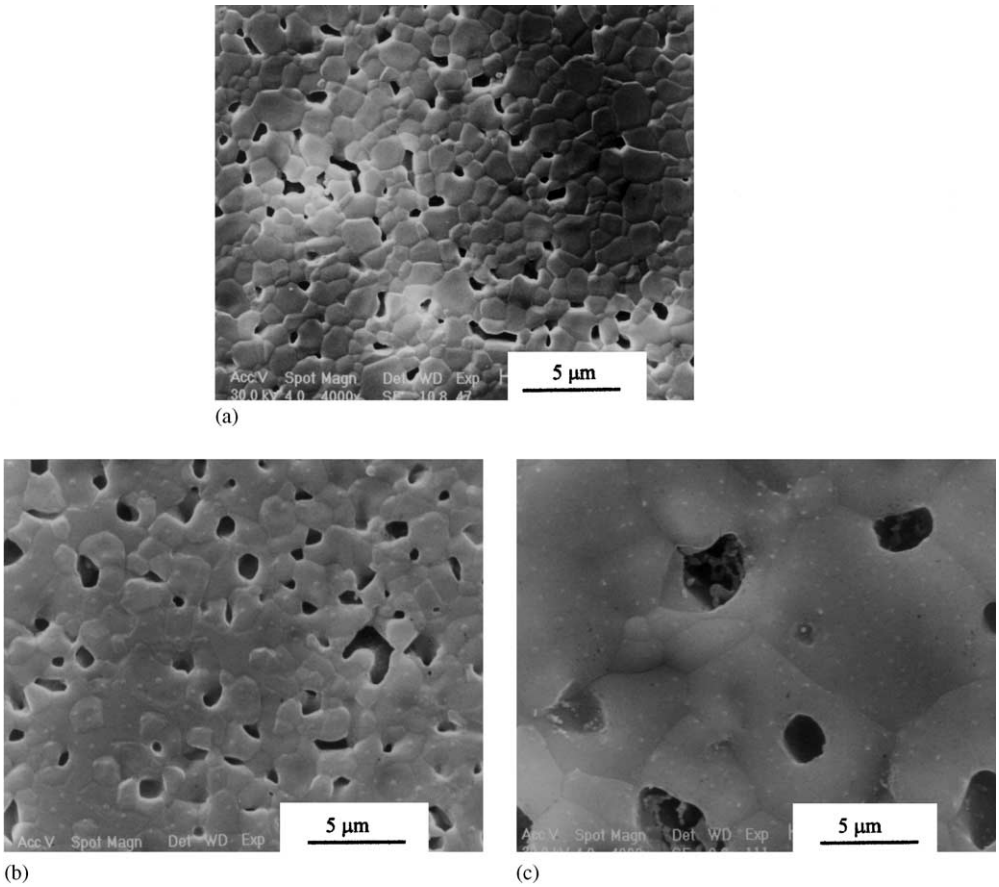

Fig. 10. SEM micrographs of sintered materials. (a) 100% HAP (Ca/P = 1.667); (b) 77% TCP + 23% HAP (Ca/P = 1.535); (c) 90% TCP + 10% $Ca_2P_2O_7$ (Ca/P = 1.44).

The microstructural observations of sintered materials showed also significant differences depending on the composition (Fig. 10). The stoichiometric HAP had an homogeneous microstructure with an average grain size of about 1 μm and the material containing CaO was similar. For biphasic systems HAP/TCP, it depended on the amount of TCP in the material. Up to 20 wt% of TCP the microstructure was close to that of pure HAP with small grains exhibiting a regular shape. On the opposite, ceramics containing a high amount of TCP (Fig. 10b and c) were characterised by coarser grains with a tortuous morphology. The presence of intragranular pores in the material with Ca/P = 1.44 (Fig. 10c) and the low densification ratio (74%) displays a strong granular coalescence as already observed during calcination below 700°C.

From these results, it appears that the development of biphasic systems HAP/TCP with powders having an initial Ca/P < 1.667 or HAP/CaO for Ca/P > 1.667 modifies noticeably the sintering of HAP based materials. The lower sinterability of biphasic compounds agrees with other works [4,13].

It can be hypothesised that the HAP/TCP materials behave as composite systems containing two phases without mutual sintering. When present in a low amount the TCP phase would act as a limiting agent of the sintering of the HAP matrix by standing in the way of diffusion on account for the decrease of the densification ratio of the material. The increase of the grain size and the drop of the densification ratio with decreasing Ca/P ratio of the initial powder must relate to the strong particle coalescence that occurs at low temperature (below 700°C) in the Ca-dHAP powder compact before the formation of the biphasic mixture. This would account for the tortuous grain morphology of HAP/TCP materials containing a high amount of TCP. In this case, the low specific surface area resulting from the low temperature coalescence reduces the reactivity and therefore the sintering ability of the material.

4. Conclusion

In this part of the study, it was shown that the sintering behaviour of biphasic calcium phosphate materials issued from Ca-dHAP $Ca_{10-x}(PO_4)_{6-x}(HPO_4)_x(OH)_{2-x}$ is greatly influenced by the initial

Ca/P ratio of the powder. During the thermal treatment, particle coalescence occurs through superficial diffusion without densification from 500°C. The particle coalescence increases with the increase of ionic vacancies concentration in the initial apatite. This coalescence may result in an important surface reduction before the beginning of the sintering that starts from 700°C, temperature at which the initial Ca-dHAP dissociates to form the biphasic HAP/TCP mixture. During sintering, biphasic compounds can be described as composites in which the minor phase slows down the sintering of the matrix. The microstructure and densification ratio of the biphasic ceramics depend on the proportions of these two phases. They can be linked to the diffusion phenomena and to the particle coalescence that occur at low temperature.

A high amount of TCP is very detrimental to the sintering of biphasic HAP/TCP ceramics. The elaboration of dense materials having a high TCP loading (>20 wt%) with controlled and fine grain microstructure by natural sintering of Ca-dHAP powders appears difficult at the present time. More investigation concerning the sintering of calcium phosphates, either HAP or TCP, is required for a better understanding of the influence of the different parameters (atmosphere, temperature, time, heating rate) on the coalescence and densification mechanisms. This work is in progress.

To overcome these difficulties, hot pressing may be used to elaborate dense materials with limited grain growth. This method was investigated to elaborate dense biphasic calcium phosphates with controlled and similar microsctructures with the aim of studying the effect of composition (HAP and TCP proportions) on the mechanical properties. The results are presented in part III of this work.

References

[1] Elliott JC, Structure and chemistry of the apatites and other calcium orthophosphates. In: Elliott JC, editor. Studies in inorganic chemistry. Amsterdam: Elsevier, 1994. p. 148–54.
[2] Ababou A, Bernache-Assollant D, Heughebaert M. Influence des conditions de calcination sur lévolution morphologique de lhydroxyapatite. Ann Chim Fr 1994;19:165–75.
[3] Asada M, Osaka A, Miura Y, Takahashi K, Oukami K, Nakamura S. Effect of Ca/P upon microstructure and sinterability of calcium hydroxyapatite. In: Somiya S, Shimasa M, Yoshimura M, Watanabe M, editors. Sintering 87. New York, 1987. p. 1326–31.
[4] Royer A, Viguie JC, Heughebaert M, Heughebaert JC. Stoichiometry of hydroxyapatite: influence on the flexural strength. J Mater Sci: Mater Med 1993;4:76–82.
[5] Fischer GR, Bardhan P, Geiger JE. The lattice thermal expansion of hydroxyapatite. J Mater Sci Lett 1983;2:577–8.
[6] Nakamura S, Otsuka R, Oaki H, Akao M, Miura N, Yamamoto T. Thermal expansion of hydroxyapatite-β-tricalcium phosphate ceramics. Thermochim Acta 1990;165:57–72.
[7] Greskovich G, Lay KW. Grain growth in very porous Al_2O_3 compacts. J Am Ceram Soc 1972;53:142–6.
[8] Ruckenstein E, Pulvermacher B. Kinetics of crystallite sintering during heat treatment of supported metal catalysts. AIChE J 1973;19:356–64.
[9] German RM, Munir ZA. Surface area reduction during isothermal sintering. J Am Ceram Soc 1976;59:379–84.
[10] Hashimoto K, Masuda T. Change in surface area of silica-alumina catalysts caused by sintering in steam atmosphere. J Chem Eng Jpn 1985;18:71–8.
[11] Gruy F. Lois dévolution de la distribution granulométrique de poudres doxydes métalliques calcinées en présence de gaz inerte. Ann Chim Fr 1993;18:69–82.
[12] Hebrard J-L, Nortier P, Pijolat M, Soustelle M. Initial sintering of submicrometer titania anatase powder. J Am Ceram Soc 1990; 73:79–84.
[13] Asada M, Oukami K, Nakamura S, Takahashi K. Microstructure and mechanical properties of non-stoichiometric apatite ceramics and sinterability of raw powder. J Ceram Soc Jpn Int Ed 1988;96:583–6.